SvedbergOpen
DISSEMINATION OF KNOWLEDGE

International Journal of Artificial Intelligence and Machine Learning

Publisher's Home Page: https://www.svedbergopen.com/

Research Paper Open Access

# Explainable AI-Driven Fault Diagnosis and Predictive Maintenance for Smart Electrical Power Systems

Meng Yuan[1*]

[1] Hangzhou City University, hangzhou. Zhejiang, 310015.China. E- mail: 19557020324@163.com
*Corresponding Author: Meng Yuan, E- mail: 19557020324@163.com

**Abstract**
Continuous and intelligent monitoring of a smart electrical power system is essential to detect faults, monitor equipment degradation, predict failure and aid timely decisions for maintenance. Most previous solutions, however, concentrate on the diagnosis of a single fault or the prediction of a condition, with the result that it cannot provide an integrated, risk-aware and explanatory maintenance support. To overcome these limitations, Recurrent Interpretable Gradient Neural Network **(**RIGNNet) is designed to carry out fault diagnosis, degradation forecasting, failure-risk estimation, maintenance prioritization and explainable decision making, all in one. It combines the following methodologies: Inception Time for multi-scale electrical fault feature extraction, Gated Recurrent Unit (GRU) for temporal dependency learning, Neural Basis Expansion Analysis for Interpretable Time Series Forecasting (N-BEATS) for future condition and degradation forecasting, Light Gradient Boosting Machine (LightGBM) for fault classification, severity assessment and failure-risk estimation, Risk-Based Maintenance Decision (RBMD) for maintenance priority and action selection and Local Interpretable Model-Agnostic Explanations (LIME) for feature-level interpretations. The system is able to detect real-time electrical measurements and equipment-condition indicators and detect abnormal patterns, predict deterioration, estimate failure risk potential and propose maintenance activities based on asset condition and criticality. The experimental results validate the effectiveness of the integrated approach for accurate fault diagnosis and predictive maintenance, which has an accuracy rate of 96.23%. In general, the methodology provides reliable, proactive, risk-informed and explainable assistance in the reliability and operational resilience of smart electrical power systems.

**Keyword:** Condition Monitoring, Fault Diagnosis, Intelligent Asset Management, Power System Reliability, Predictive Maintenance and Smart Electrical Power Systems.

## 1. Introduction

Intelligent solutions are needed for smart electrical power systems, which should continuously monitor the condition of equipment, detect new faults, be able to forecast the degradation and failure risk and aid in making maintenance decisions in time. Current AI-based methods, however, tackle only a single task and require a more holistic method that incorporates fault diagnosis, degradation prediction, failure-risk estimation, maintenance decision-making and explainability. A hybrid Machine Learning (ML) method was proposed to predict transformer failures with the use of Internet of Things (IoT) monitoring and Explainable Artificial Intelligent (XAI), however, it did not have the capability to make transformer degradation predictions and risk-based maintenance [1]. Another Artificial Intelligent (AI) optimization method focused on predictive maintenance and cyber security, rather than both explanatory and fault diagnosis [2]. A machine-transmission line ensemble-learning approach was used to classify transmission-line faults using PMU data and XAI, but it did not include degradation prediction and maintenance prioritization [3]. An explainable quantum deep neural network was used to detect faults in DC microgrids without considering degradation forecasting or predictive maintenance [4]. Hybrid Convolutional Neural Network (CNN) decision tree for the transmission line fault classification using XAI without taking into account the lifecycle condition prediction [5]. A Random Forest–XGBoost model identified wind turbine faults, but did not have built-in maintenance prioritization [6]. A CNN-Transformer model was developed for transmission line fault classification without considering the degradation or failure risk assessment [7]. Optimised Machine Learning (ML) models were used for fault detection and localization in the power grid, but were not used for degradation forecasting and maintenance recommendations [8]. There were some attempts to implement machine-learning methods for smart-grid fault detection, but not to include degradation prediction and decisions on maintenance [9]. A Deep Learning (DL) technique was used to identify faults from PMU images but did not include degradation prediction and risk-based maintenance planning [10]. A hybrid machine and DL algorithm was used to conduct multi-stage fault diagnosis and did not predict machine degradation or provide explanations for maintenance decisions [11]. There was a hybrid machine-learning approach to fault prediction in RIS, but it was not explainable and prioritizes maintenance [12]. Machine-learning models have been tested for transmission fault diagnosis with renewable integration, but have not yet been used for degradation forecasting and predictive maintenance [13]. For the power grid, DL algorithms have been applied to fault detection, without the estimation of the risk of failure or the decision of maintenance [14]. The transmission-line fault diagnosis was modeled by DL with Long Short Term Memory (LSTM) autoencoders, but did not include the prediction of degradation and risk-based maintenance [15]. A light-weight multi-scale CNN was used to classify transformer faults but did not consider fault degradation and maintenance decisions [16]. However, smart-grid fault diagnosis was achieved with the use of tensor computing and meta-learning but without failure-risk estimation and explainable maintenance planning [17]. A hybrid deep-learning approach assisted real-time microgrid faults management, but did not provide degradation forecasting and maintenance prioritization [18]. DL and Kalman filtering were used to diagnose reactive-power fault, which was different from degradation and prediction maintenance [19]. Power-equipment fault detection was achieved by transformer-based transfer learning from images, but was not continuous and not based on degradation [20]. The Recurrent Interpretable Gradient Neural Network (RIGNNet) addresses all these limitations by solving joint problems of fault diagnosis, degradation prediction, failure-risk estimation, maintenance prioritization and explainable decision-making. It used to identify abnormal conditions of the equipment at an early stage, allows for prompt maintenance activities and provides clear information for the reliable operation of the power system. The main contributions of this research are summarized as follows:

- Develops RIGNNet for accurate identification and classification of emerging faults from electrical and condition-monitoring data.
- Predicts equipment deterioration and failure potential and used to identify critical assets at an early stage.
- Prioritises maintenance and propose appropriate maintenance based on equipment condition and risk level.
- Provides clear descriptions of model forecasts enabling operators to grasp the most important aspects of the fault and maintenance decision making process.

The research is organized as follows: Section 2 introduces the background study and research gap, Section 3 explains the proposed RIGNNet methodology and Section 4 shows the experimental results. Section 5 discusses the ablation, deployment and limitations, while Section 6 concludes the research with future work.

## 2. Background Study

Zhang et al. (2026) [21] proposed the imbalanced O&M logs diagnosis method by combining BERT-BiLSTM-CRF with BERT-MLP, knowledge graph and RAG-based reasoning. This is a new method that would enhance a more interpretable diagnosis and would still focus on textual fault records, without the same type of continuous electrical-condition monitoring.

Yang et al. (2025) [22] proposed a GAF-based dual-channel CNN, which is constructed by two CNNs, one for the GASF and another for the GADF image. The method performed high accuracy of diagnosis, but mostly dealt with fault classification, not degradation prediction and/or maintenance decisions.

Xiao et al. (2026) [23] developed an NA-MEMD and modified multiple-branch CNN method for the detection and classification of distribution-network faults. It was effective in the approach and able to represent nonlinear fault signals, but only for the diagnosis and not predictive maintenance with explainable decisions.

Jachymczyk et al. (2024) [24] proposed an intelligent condition-monitoring method for condition-based predictive maintenance that involves diagnostic-indicator selection. The method eliminated the unnecessary indicators, but due to its equipment-specific nature, it could not be generalized to a more general smart electrical power system.

Abdolahi et al. (2025) [25] analyzed the potential of advanced machine-learning models for power-cable condition monitoring using electrical health indicators. The prediction performance of the models was satisfactory, but fault diagnosis, explainability and decisions for maintenance action were not optimized together.

Hamalainen et al. (2025) [26] developed a deep-learning condition-monitoring method for quickly deploying models to rotating machines and operating conditions. Although condition monitoring was effective, the approach was mainly diagnosis and not degradation forecasting and maintenance prioritisation.

Long et al. (2026) [27] proposed CNN-BiGRU-Attention based recurrent plots for the transmission line fault diagnosis, which enhanced the representation of time-frequency characteristics and noise immunity. The research focused on fault identification, however and no attempt was made to incorporate failure-risk prediction or make maintenance decisions.

Li and Wu (2026) [28] proposed an enhanced CNN-BiGRU method for fault-type identification for distribution networks with distributed power sources. While adaptability under distributed-generation conditions was improved, degradation forecasting, predictive maintenance and explainable maintenance recommendations were not addressed.

**Table 1: Recent Advances in Intelligent Power-System Fault Detection and Condition Prediction**

| Author (Year) | Concept | Method Used | Limitation | Result |
|---|---|---|---|---|
| Zhang et al. (2025)[29] | Short-term load forecasting | K-Shape + DL | Did not address fault diagnosis or maintenance | Improved load forecasting |
| Aravanis and Kanavos (2026)[30] | Electricity-demand forecasting | Comparative deep-learning models | Did not address faults or maintenance | Identified effective forecasting architectures |
| Nawaz et al. (2025)[31] | Transmission-line fault diagnosis | Gradient-boosting feature selection | No degradation or maintenance prediction | Improved feature selection and diagnosis |
| Nawaz et al. (2026)[32] | UHV transmission fault diagnosis | Consensus feature selection + Bayesian stacking | Computationally complex; diagnosis-focused | Improved comprehensive fault diagnosis |
| Oliveira et al. (2024)[33] | Electrical fault detection | Multiple classifier systems | No degradation or maintenance decisions | Improved fault detection |
| Chen et al. (2024)[34] | DC charging-station fault diagnosis | S-Transform + LightGBM | Limited to open-circuit faults | Effectively detected open-circuit faults |
| Choi and Joe (2025)[35] | Electrical-machine fault diagnosis | Frequency-aware Transformer | No maintenance prioritization | Improved multiscale fault diagnosis |

Table 1 summarizes recent AI-based methods for fault detection, diagnosis, feature selection and condition prediction in power system, highlighting its methods, limitations and results. The researches reviewed stress the importance of an integrated solution combining the aspects of fault diagnosis, degradation prediction, failure risk assessment, maintenance decisions and explainability.

### 2.1 Research Gap

Most of the existing research focused on individual fault detection, fault classification, condition monitoring, or load forecasting, but integrated degradation prediction, failure-risk assessment, maintenance prioritization and explainability were limited. Most methods were application dependent and did not provide a common method of dealing with time-related electrical measurements and changing conditions of the equipment. The proposed RIGNNet combines the benefits of InceptionTime, GRU, N-BEATS, LightGBM, RBMD and LIME to provide a comprehensive solution for fault diagnosis, degradation forecasting, risk estimation and maintenance decision making. The integrated design enhances the ability to detect faults early, to predict failures, to prioritize the assets and to make transparent decisions for smart electrical power systems.

## 3. Proposed Methodology

This section discusses the architecture with all the integrated processes of fault diagnosis, temporal analysis, degradation forecasting, risk prediction, maintenance decision-making and explainability. The mathematical equations and the pseudo code give details of the computational operations and the overall procedure for implementation.

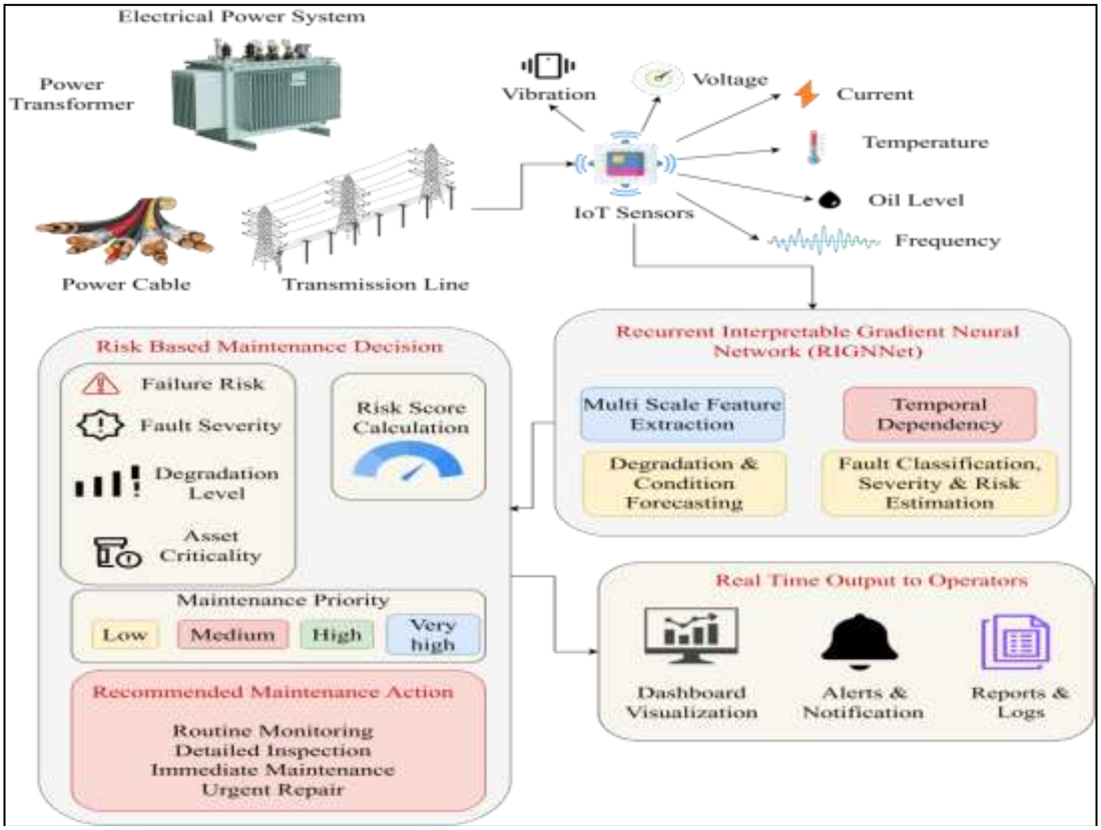


**Figure 1: RIGNNet-Based Intelligent Fault Diagnosis and Risk-Based Maintenance Decision Support**

The figure 1 shows the working of RIGNNet in extracting multiple-scale features, analyzing the data over time, forecasting equipment degradation, classification of faults, severity and risk estimation of the degradation states. The outputs of the risk-based maintenance module are used to generate the maintenance priorities and recommended actions for the operators to be provided in real time via dashboards, alerts, reports and logs.

### 3.1 Dataset Description

The Large Power Transformer Maintenance Dataset is used as the benchmark dataset for testing the intelligent transformer condition detection and maintenance prediction. It contains 7,500 samples of transformers that have been monitored and 18 features derived from the sensors in addition to a label that indicates the time it require maintenance. The data includes the temperature of the LTC oil, the main-tank oil and the temperature of the dissolved gases, which are indicative of the condition of the transformer during operation and the state of the transformer's health. It allows assessing the conditions, analyzing faults, estimating failure risks and conducting researches on predictive maintenance.

### 3.2 Data Preprocessing

Collected transformer monitoring data is cleaned to eliminate inconsistent data, duplicate records and invalid measurements. This can be made compatible with the learning models by filling in the missing values in numerical variables and encoding the different categories of the categorical variables. All numerical features are scaled in the same range and the data is divided into train/validation/test sets with the distribution of maintenance condition kept. These steps used to enhance data quality, ensuring accurate model training and evaluation.

### 3.3 Recurrent Interpretable Gradient Neural Network (RIGNNet)

RIGNNet is an envisioned intelligent approach to real-time fault diagnosis and predictive maintenance in smart electrical power systems based on InceptionTime, Gated Recurrent Unit (GRU), Neural Basis Expansion Analysis for Interpretable Time Series Forecasting (N-BEATS), Light Gradient Boosting Machine (LightGBM), Risk-Based Maintenance Decision (RBMD) and Local Interpretable Model-Agnostic Explanations (LIME). GRU infers the temporal dependence and evolvement of the abnormal pattern, while InceptionTime extracts the multi-scale fault features. The N-BEATS forecasts degradation of equipment and operating conditions in the future and LightGBM classifies faults and estimates the level of fault or the risk of equipment failure. The probability of failure, the severity of the fault and its degradation level are combined in the RBMD layer, which is used to prioritise maintenance activities as well as to propose maintenance actions based on the criticality of the asset. LIME is transparent and shows which of the most important electrical and operational parameters influences each prediction. The methodology can be used to identify and diagnose faults, predict fault degradation, estimate failure risks, condition-based maintenance and prioritize assets and explainable decision making. Its modular design can allow for a variety of assets including power cables, circuit breakers, transformers and transmission lines to be accommodated. Defining the data sets and partitioning it into fixed sets and documenting hyper parameters and evaluation process can make it easier to assure reproducibility. Overall, RIGNNet overcomes the disadvantages of individual diagnosis methods by combining the use of fault analysis, temporal forecasting, risk estimation, maintenance decision-making and explainability to benefit the reliable monitoring and maintenance of power systems.

$$X' = \frac{X-\mu}{\sigma} \tag{1}$$

This equation (1) represents the normalization of electrical and condition-monitoring measurements for consistent model processing. Here, $X$ denotes the original measurement, $\mu$ represents the mean value, $\sigma$ denotes the standard deviation and $X'$ represents the normalized measurement.

$$F_k = \sigma(W_k * X + b_k) \tag{2}$$

This equation (2) represents multi-scale feature extraction using an InceptionTime convolutional branch. Here, $X$ denotes the input signal, $W_k$ represents the convolution kernel of branch $k$, $b_k$ denotes the bias, $*$ represents convolution, $\sigma$ denotes the activation function and $F_k$ represents the extracted feature.

$$F = \text{Concat}(F_1, F_2, \dots, F_K) \tag{3}$$

This equation (3) represents the fusion of features obtained from multiple InceptionTime branches. Here, $F_1, \dots, F_K$ denote the features extracted at different scales, $K$ represents the number of branches and $F$ denotes the combined feature representation.

$$z_t = \sigma(W_z X_t + U_z h_{t-1}) \tag{4}$$

This equation (4) represents the GRU update gate for controlling how much previous information is retained. Here, $X_t$ denotes the current input, $h_{t-1}$ represents the previous hidden state, $W_z$ and $U_z$ are learnable weight matrices and $z_t$ denotes the update gate.

$$r_t = \sigma(W_r X_t + U_r h_{t-1}) \tag{5}$$

This equation (5) represents the GRU reset gate for controlling the influence of previous information on the current state. Here, $X_t$ denotes the current input, $h_{t-1}$ represents the previous hidden state, $W_r$ and $U_r$ are learnable weights and $r_t$ denotes the reset gate.

$$\tilde{h}_t = \tanh\left(W_h X_t + U_h (r_t \odot h_{t-1})\right) \tag{6}$$

This equation (6) represents the generation of the candidate hidden state in the GRU. Here, $X_t$ denotes the current input, $h_{t-1}$ represents the previous hidden state, $W_h$ and $U_h$ are learnable weights, $r_t$ is the reset gate and $\odot$ denotes element-wise multiplication.

$$h_t = (1 - z_t) h_{t-1} + z_t \tilde{h}_t \tag{7}$$

This equation (7) represents the updated GRU hidden state by combining previous and current information. Here, $h_t$ denotes the current hidden state, $h_{t-1}$ represents the previous hidden state, $z_t$ is the update gate and $\tilde{h}_t$ denotes the candidate state.

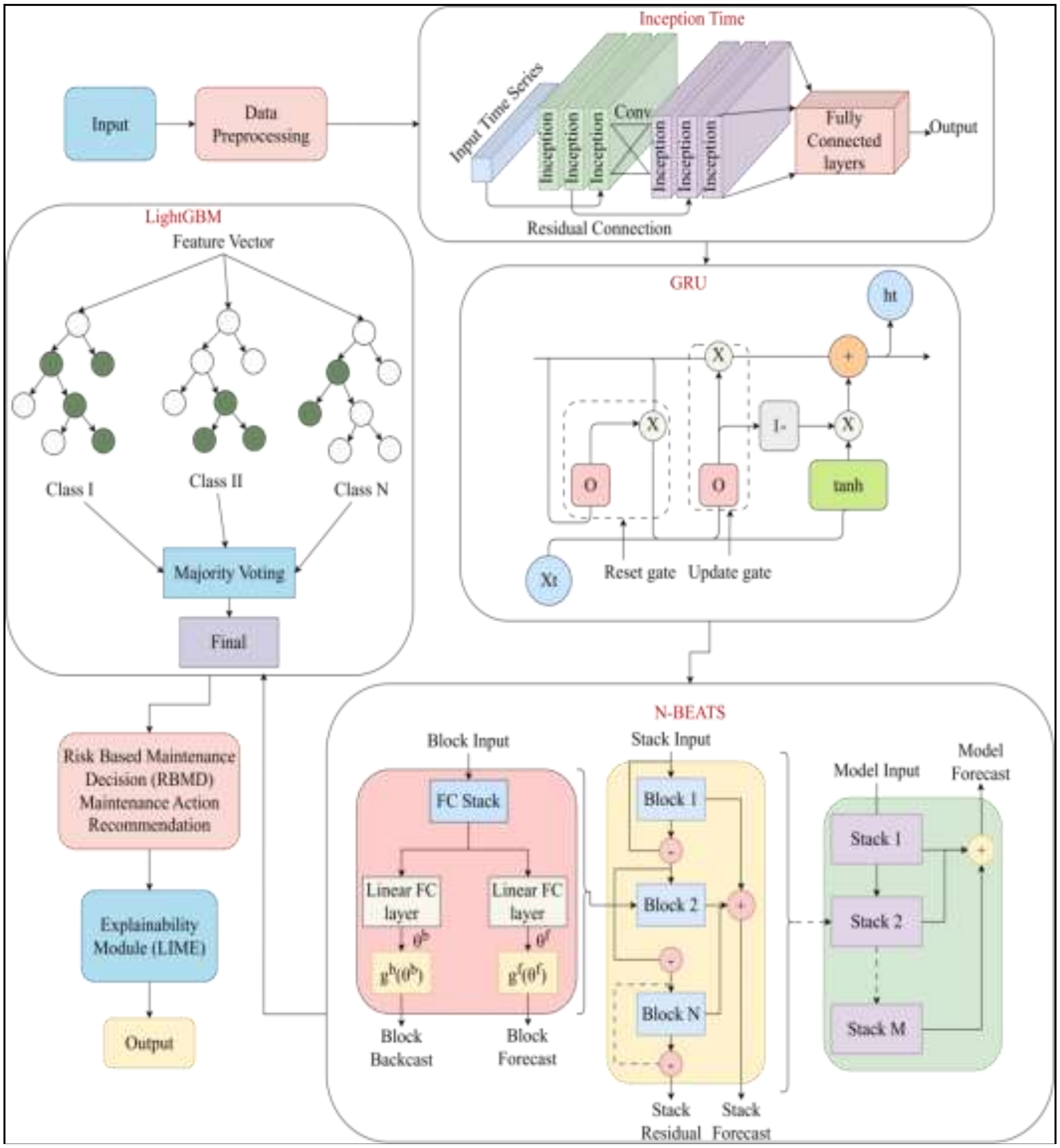


**Figure 2: Architecture of the Proposed RIGNNet**

The figure 2 illustrates a real-time data flow of equipment-condition data to RIGNNet for multi-scale feature extraction and temporal analysis, equipment-degradation forecasting, fault classification, severity and risk estimation. The outputs of the risk based maintenance module are translated to maintenance priorities and recommended action which are available as real-time dashboards, alerts, reports and logs to the operators.

### 3.4 Intelligent Fault Diagnosis and Temporal Condition Analysis

InceptionTime is a tool that is able to calculate multi-scale signatures of faults from real-time electrical measurements and condition data of the equipment. GRU can learn temporal-dependencies and changing abnormal operating patterns between subsequent observations. The integrated models are designed to identify faults in the system and to categorize the different fault types, based on the learned signal characteristics. Temporal analysis can detect abnormal operation of equipment in early stage before it turns to be unprecedented failure. The diagnostic information generated is then utilised for degradation and failure risk prediction.

$$\theta = g(h_t) \tag{8}$$

This equation (8) represents the transformation of the temporal feature representation into N-BEATS parameters. Here, $h_t$ denotes the GRU temporal representation, $g(\cdot)$ represents the N-BEATS block and $\theta$ denotes the learned basis coefficients.

$$\hat{X}_t = \theta^b B \tag{9}$$

This equation (9) represents the reconstruction of the observed input sequence using the N-BEATS backcast component. Here, $\theta^b$ denotes the backcast coefficients, $B$ represents the backcast basis and $\hat{X}_t$ denotes the reconstructed input.

$$\hat{Y}_{t+h} = \theta^f F_h \quad (10)$$

This equation (10) represents future-condition forecasting using the N-BEATS forecast component. Here, $\theta^f$ denotes the forecast coefficients, $F_h$ represents the forecast basis at horizon $h$ and $\hat{Y}_{t+h}$ denotes the predicted future condition.

$$L_f = \left(Y - \hat{Y}\right)^2 \quad (11)$$

This equation (11) represents the forecasting error used to measure the difference between actual and predicted equipment conditions. Here, $Y$ denotes the actual condition value, $\hat{Y}$ represents the predicted value and $L_f$ denotes the forecasting loss.

$$\hat{y} = \sum m = 1M\eta\, f_m(X) \quad (12)$$

This equation (12) represents the LightGBM prediction obtained by combining multiple decision trees. Here, $X$ denotes the input features, $f_m$ represents the $m$-th decision tree, $M$ denotes the total number of trees, $\eta$ represents the learning rate and $\hat{y}$ denotes the final prediction.

$$P_c = \frac{e^{s_c}}{\sum je^{s_j}} \quad (13)$$

This equation (13) represents the probability assigned to a particular fault class. Here, $s_c$ denotes the prediction score for fault class $c$, $j$ represents all possible fault classes and $P_c$ denotes the probability of class $c$.

### 3.5 Equipment Degradation and Failure-Risk Prediction

N-BEATS predicts future operating conditions and degradation of equipment in the monitored power system using the predicting of time series. LightGBM is able to detect faults and label it, determine the fault severity and the risk of failure. The predictions can be combined to provide early detection of assets operating in close proximity to critical operating conditions. The failure-risk score can be used in prioritizing equipment according to failure risk and condition-based maintenance planning. Thereby, miscellaneous outages and maintenance actions can be avoided.

$$R_f = P(\text{failure} \mid X) \quad (14)$$

This equation (14) represents the estimated probability of equipment failure based on the observed condition data. Here, $X$ denotes the monitored electrical and operational features and $R_f$ represents the estimated failure risk.

$$D = 1 - \frac{RUL}{RUL_{\max}} \quad (15)$$

This equation (15) represents the normalized degradation level of the equipment. Here, $RUL$ denotes the predicted remaining useful life, $RUL_{\max}$ represents the maximum reference useful life and $D$ denotes the degradation index.

$$S_f = \sum iw_i\, f_i \quad (16)$$

This equation (16) represents the overall fault severity based on relevant condition indicators. Here, $f_i$ denotes the $i$-th fault-related indicator, $w_i$ represents its corresponding importance weight and $S_f$ denotes the overall severity score.

$$R = \alpha R_f + \beta D + \gamma S_f \quad (17)$$

This equation (17) represents the overall maintenance risk score by combining failure probability, degradation and fault severity. Here, $R_f$ denotes failure risk, $D$ represents degradation, $S_f$ denotes fault severity and $\alpha, \beta, \gamma$ are weighting coefficients.

### 3.6 Explainable Risk-Based Maintenance Decision Support

RBMD provides failure risk prediction, fault severity, degradation level and asset criticality and based on this, it sets maintenance priority and then recommends the appropriate maintenance action. LIME documents the important electrical and operating characteristics that impact each prediction, giving clear explanations for the maintenance actions that are taken. The explanations enable operators to comprehend why the asset has a specific maintenance priority and why an intervention is recommended. The integrated approach allows for informed condition-based maintenance, adds transparency in decision making and boosts the practical applicability of RIGNNet for reliable monitoring and maintenance of smart power systems.

$$MP = \begin{cases} High, & R \geq \tau \\ Low, & R < \tau \end{cases} \quad (18)$$

This equation (18) represents the assignment of maintenance priority according to the calculated risk score. Here, $R$ denotes the maintenance risk score, $\tau$ represents the predefined risk threshold and $MP$ denotes the maintenance priority.

$$A^* = \text{argmax}_A U(A|R) \quad (19)$$

This equation (19) represents the selection of the most suitable maintenance action according to the estimated risk. Here, $A$ denotes a possible maintenance action, $U(A|R)$ represents its utility under risk condition $R$ and $A^*$ denotes the selected maintenance action.

$$\xi = \text{argmin}_g [L(f, g) + \Omega(g)] \quad (20)$$

This equation (20) represents the generation of a local interpretable explanation for the model prediction. Here, $f$ denotes the original RIGNNet prediction model, $g$ represents the interpretable local model, $L(f, g)$ denotes the difference between the original and local predictions, $\Omega(g)$ represents the complexity penalty and $\xi$ denotes the resulting explanation.

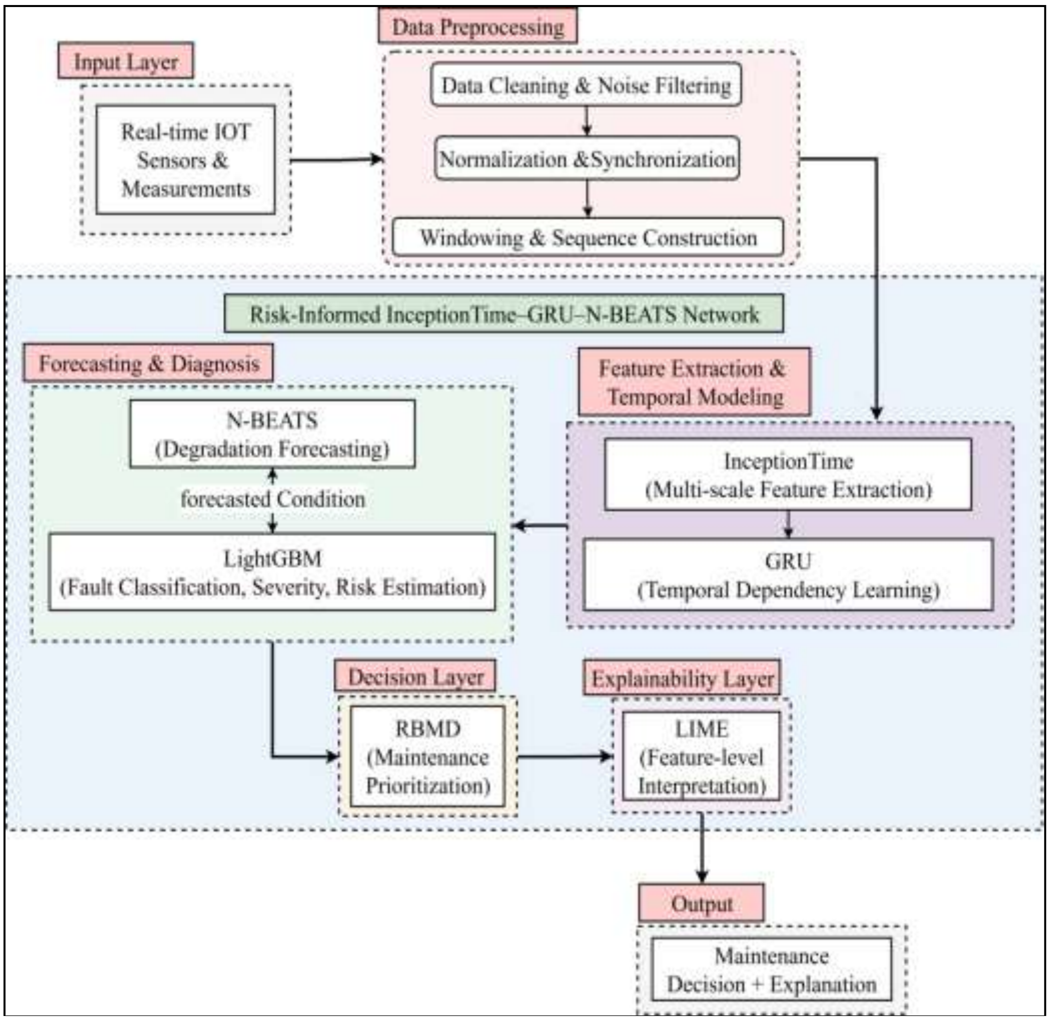


**Figure 3: Algorithm Workflow of the Proposed RIGNNet**

Figure 3 shows the overall flow of the proposed **RIGNNet** for multimodal NDE-based defect detection, classification, severity assessment and quality evaluation. This end-to-end process entails feature extraction, explainable decision making, attention-based detection and reinforcement learning to optimize manufacture adaptively.

| **Algorithm: Recurrent Interpretable Gradient Neural Network (RIGNNet)** |
| --- |
| Input:<br>X ← Transformer condition-monitoring data<br>Yf ← Fault-condition labels |

Ym ← Maintenance-required labels
E ← Number of training epochs
Begin
Load X, Yf and Ym from the benchmark dataset.
Normalize the numerical measurements:
$X' \leftarrow (X - \mu) / \sigma$
Extract multi-scale features using InceptionTime:
$Fk \leftarrow Activation(Wk * X' + bk)$
Fuse the multi-scale features:
$F \leftarrow Concatenate(F1, F2, \dots, FK)$
Learn temporal dependencies using GRU:
$zt \leftarrow UpdateGate(Ft, ht - 1)$
$rt \leftarrow ResetGate(Ft, ht - 1)$
$\tilde{h}t \leftarrow CandidateState(Ft, rt, ht - 1)$
$ht \leftarrow GRUState(zt, \tilde{h}t, ht - 1)$
Generate temporal representations:
$\theta \leftarrow N - BEATS(ht)$
Forecast future equipment condition:
$\hat{Y}t + h \leftarrow N - BEATS\_Forecast(\theta)$
Calculate degradation:
$D \leftarrow 1 - RUL/RULmax$
Train LightGBM using learned features and forecast indicators:
$\hat{y}f \leftarrow LightGBM(F, ht, \hat{Y}t + h, D)$
Determine the fault class:
$FaultClass \leftarrow argmax(Pc)$
Estimate fault severity:
$Sf \leftarrow \Sigma\, wi\, fi$
Estimate failure risk:
$Rf \leftarrow P(Failure \mid X)$
Calculate the maintenance risk score:
$R \leftarrow \alpha Rf + \beta D + \gamma Sf$
Determine maintenance priority:
If R ≥ τ:
MP ← High
Else:
MP ← Low
Select the maintenance action:
$A * \leftarrow argmax\ U(A \mid R)$
Generate local explanations using LIME:
$\xi \leftarrow LIME(LightGBM, X)$
Return:
$FaultClass, Sf, D, Rf, MP, A *, \xi$
End Algorithm
Output:
Fault class
Failure risk
Recommended maintenance action

The RIGNNet pseudo code processes transformer condition-monitoring data through InceptionTime, GRU, N-BEATS and LightGBM to identify faults, estimate severity, predict degradation and assess failure risk. The RBMD component determines maintenance priority and suitable actions, while **LIME** explains the key features influencing each prediction for transparent decision-making.

## 4. Experiment Results

This section assesses the performance of RIGNNet for fault diagnosis, severity assessment, degradation prediction, failure-risk estimation and maintenance decision making. Its experimental results confirm its accuracy, reliability, capability of prediction and consistency over various operating conditions.

The condition-monitoring data set for the transformer was split into a 70% training data set, 15% validation data set and 15% test data set, with the same distribution of fault and maintenance data sets. The input features for RIGNNet were normalized with min–max normalization and sequential observations were temporally aligned prior to building RIGNNet inputs. Multi-scale fault features were extracted by InceptionTime, temporal dependencies were learned by GRU and future equipment conditions and degradation trends were forecasted by N-BEATS. LightGBM was used for fault classification, fault severity and failure risk determination, while RBMD was used for maintenance priority and proper maintenance actions based on failure risk, degradation, asset criticality and fault severity. LIME provided local explanations of the resulting predictions. Adam optimization is used to train RIGNNet with a learning rate of 0.001, batch size of 64 and 150 epochs with learning-rate scheduling and early stopping for better convergence. The experiments were carried out on an Intel Core i9-13900K workstation with 32 GB of DDR5 memory and an NVIDIA RTX 4090 GPU (24 GB VRAM) using Windows 11 Pro. The model was implemented in Python 3.10, PyTorch 2.2 with CUDA 12.1. To ensure reproducibility, all experiments were conducted under the same set of configurations enabling the reliable evaluation of the results based on Accuracy, Precision, Recall, F1-Score, RMSE and ROC-AUC.

**Table 2: Numerical Distribution of Electrical Fault Classes**

| Fault Class | Fault Code | Sample Count | Voltage Range (kV) | Current Range (A) | Frequency (Hz) |
|---|---|---|---|---|---|
| Normal | 0 | 1,250 | 10.8–11.2 | 85–125 | 49.8–50.2 |
| Line-to-Ground | 1 | 840 | 8.6–10.4 | 145–280 | 49.5–50.1 |
| Line-to-Line | 2 | 720 | 8.2–10.1 | 165–310 | 49.4–50.0 |
| Double-Line-to-Ground | 3 | 615 | 7.5–9.8 | 190–345 | 49.2–49.9 |
| Three-Phase | 4 | 530 | 6.9–9.2 | 225–390 | 49.0–49.8 |
| Open-Circuit | 5 | 465 | 9.1–10.7 | 35–90 | 49.6–50.1 |

Table 2 shows the distribution of the number of samples in each electrical fault class, by voltage, current and frequency ranges. The results reveal that the fault condition has an influence on the current and the voltage and frequency drops as compared to normal condition.

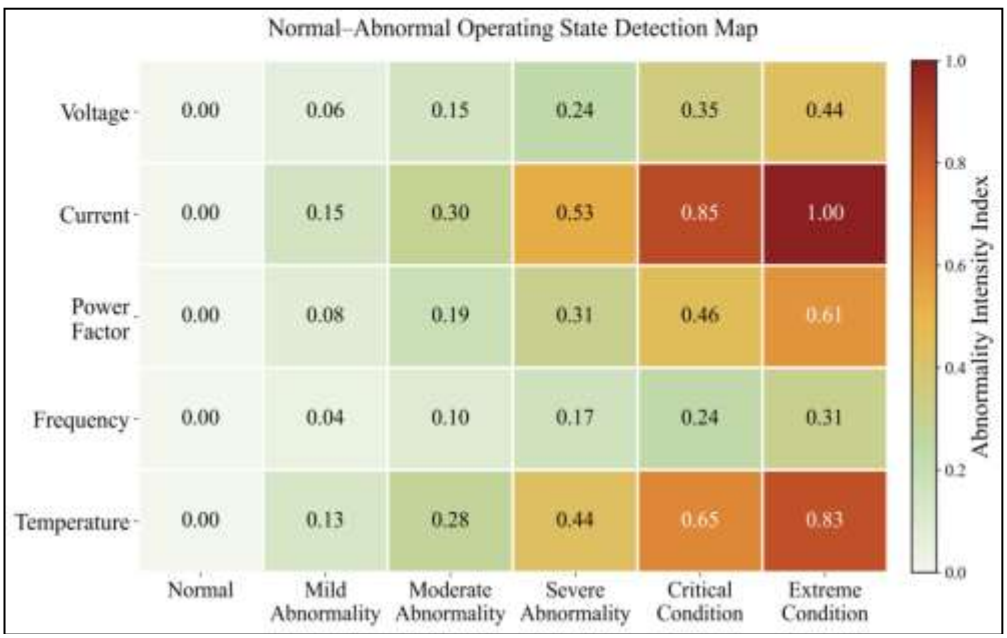


**Figure 4: Normal–Abnormal Operating State Detection Map**

The Figure 4 depicts the distribution of normal and abnormal operating states, by electrical condition variable and observation period. It identifies areas that show abnormal behavior as a result of combinations of certain operating conditions.

**Table 3: Numerical Electrical Condition Indicators for Fault Diagnosis**

| Condition | Voltage (kV) | Current (A) | Power Factor | Frequency (Hz) | Temperature (°C) |
|---|---|---|---|---|---|
| Normal | 11.05 | 105 | 0.96 | 50.02 | 58 |
| Mild abnormality | 10.72 | 138 | 0.93 | 49.94 | 64 |
| Moderate abnormality | 10.31 | 176 | 0.89 | 49.81 | 71 |
| Severe abnormality | 9.74 | 225 | 0.83 | 49.65 | 79 |
| Critical condition | 8.92 | 290 | 0.76 | 49.42 | 88 |
| Extreme condition | 8.15 | 345 | 0.69 | 49.21 | 96 |

Table 3 shows the differences in important electrical and thermal measurements under varying conditions. When the condition moves from normal to extreme, the voltage and power factor decline and the current and temperature rise, showing the conditions of the equipment are getting worse.

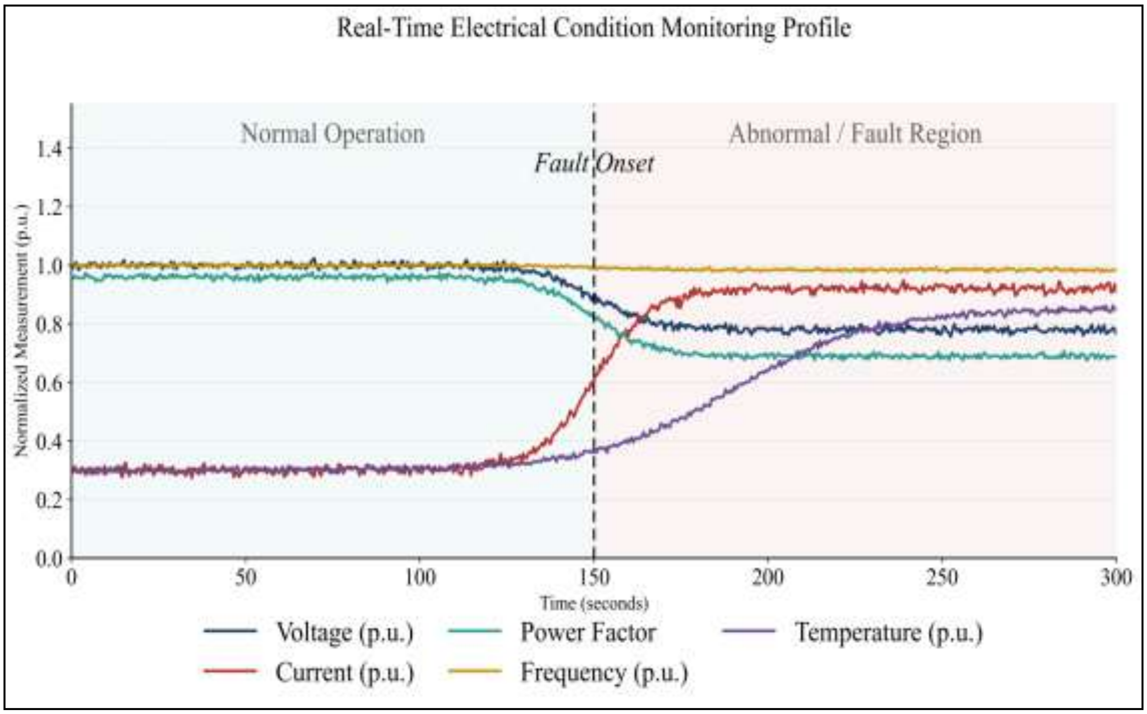


**Figure 5: Real-Time Electrical Condition Monitoring Profile**

The figure 5 shows the temporal changes of the main electrical parameters, such as voltage, current, frequency, power factor and temperature during system operation. It gives an ongoing display of the condition of the electrical system for early detection of abnormal operating conditions.

**Table 4: Fault Severity Levels and Numerical Indicators**

| Severity Level | Severity Score | Current Increase (%) | Voltage Deviation (%) | Temperature Increase (°C) | Condition |
|---|---|---|---|---|---|
| Normal | 0.05 | 2 | 1 | 2 | Healthy |
| Very Low | 0.18 | 6 | 3 | 5 | Minor |
| Low | 0.32 | 12 | 5 | 9 | Early fault |
| Moderate | 0.51 | 21 | 8 | 15 | Developing fault |
| High | 0.74 | 34 | 13 | 23 | Severe fault |
| Critical | 0.93 | 48 | 19 | 34 | Critical fault |

Numerical severity scores as per current increase, voltage deviation and temperature rise are given in Table 4. The increasing values along severity levels show the progressive condition of the fault - from the healthy operation to the critical fault.

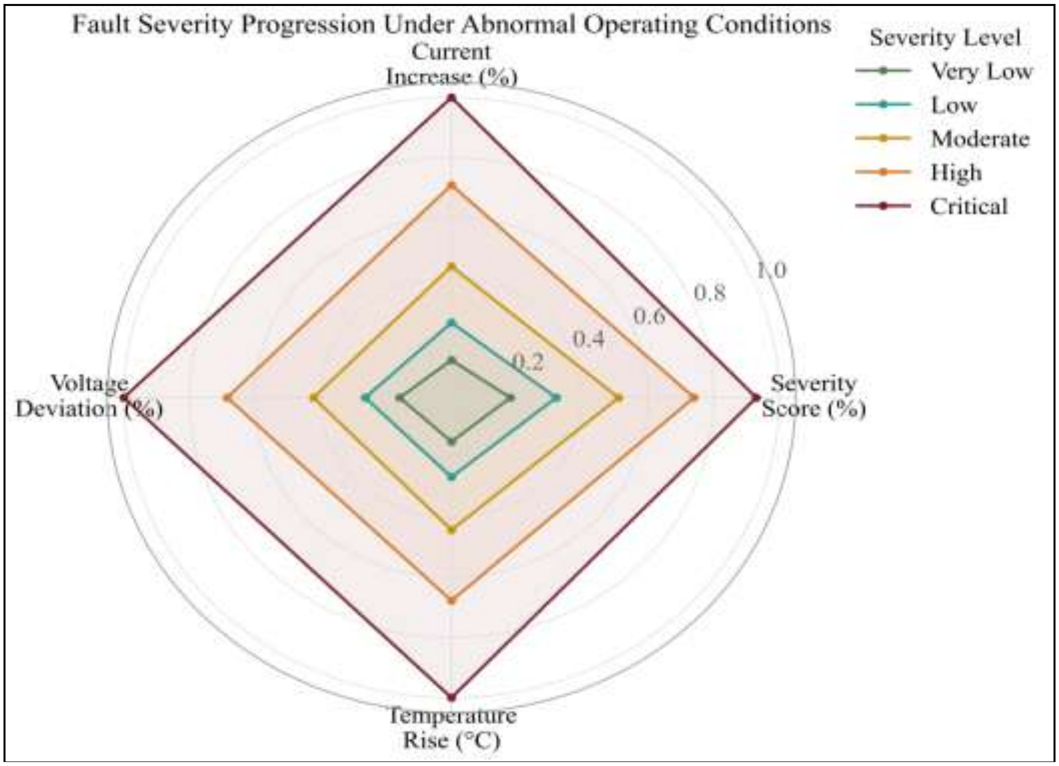


**Figure 6: Fault Severity Progression Under Abnormal Operating Conditions**

Figure 6 shows the growth of fault severity for several electrical condition indicators. It is a representative example of how a progressive increase in abnormality is manifested as a voltage deviation, an increase in current and a change in the other abnormality severity factors.

**Table 5: Predicted Equipment Degradation Levels**

| Asset ID | Operating Age (Years) | Predicted RUL (Months) | Degradation Index | Load Level (%) | Condition Level |
|---|---|---|---|---|---|
| A01 | 2 | 118 | 0.08 | 54 | Healthy |
| A02 | 4 | 94 | 0.21 | 61 | Slight degradation |
| A03 | 6 | 76 | 0.36 | 68 | Moderate degradation |
| A04 | 8 | 57 | 0.52 | 74 | Noticeable degradation |
| A05 | 11 | 34 | 0.71 | 82 | Severe degradation |
| A06 | 14 | 16 | 0.87 | 91 | Critical degradation |

Table 5 shows the predicted degradation status of various assets based on operating age, RUL, degradation index and load level. The greater the operating age and load, the less the RUL and the higher the degradation index, which means that the equipment has been deteriorating every day.

**Table 6: Future Equipment Condition Forecast**

| Forecast Horizon | Temperature (°C) | Load (%) | Insulation Index | Vibration (mm/s) | Predicted Condition |
|---|---|---|---|---|---|
| 1 Month | 61 | 68 | 0.94 | 1.8 | Healthy |
| 3 Months | 64 | 71 | 0.91 | 2.1 | Healthy |
| 6 Months | 69 | 75 | 0.86 | 2.7 | Slight degradation |
| 9 Months | 74 | 79 | 0.80 | 3.4 | Moderate degradation |

| | | | | | |
|---|---|---|---|---|---|
| 12 Months | 81 | 84 | 0.72 | 4.3 | High degradation |
| 15 Months | 89 | 91 | 0.61 | 5.6 | Critical condition |

Table 6 presents the projected equipment condition over the next three years based on the temperature, load, insulation and vibration indicators. The higher the temperature, load and vibration, the lower the insulation index which reflects a gradual progression toward unhealthy to critical conditions.

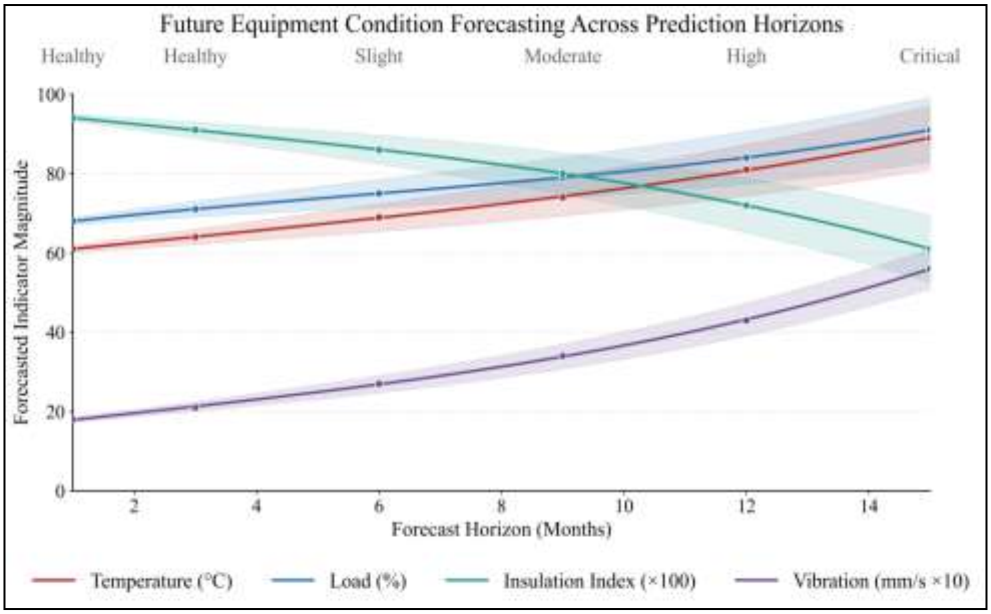


**Figure 7: Future Equipment Condition Forecasting Across Prediction Horizons**

Figure 7 shows the evolution of equipment condition over several future time horizons. It illustrates how indicators of an operation are changing over time, giving a warning of future deterioration.

**Table 7: Numerical Failure-Risk Prediction**

| Asset | Failure Probability | Degradation Index | Fault Severity | Failure-Risk Score | Risk Level |
|---|---|---|---|---|---|
| A01 | 0.06 | 0.08 | 0.10 | 0.08 | Very Low |
| A02 | 0.14 | 0.21 | 0.18 | 0.17 | Low |
| A03 | 0.29 | 0.36 | 0.34 | 0.32 | Moderate |
| A04 | 0.46 | 0.52 | 0.49 | 0.49 | Medium |
| A05 | 0.68 | 0.71 | 0.73 | 0.71 | High |
| A06 | 0.91 | 0.87 | 0.92 | 0.90 | Critical |

Table 7 shows failure probability, degradation index, fault severity and overall failure-risk scores for various assets. A higher degradation score coupled with a higher fault severity score means that the score for failure risk is higher and certain assets with greater failure risk can be identified.

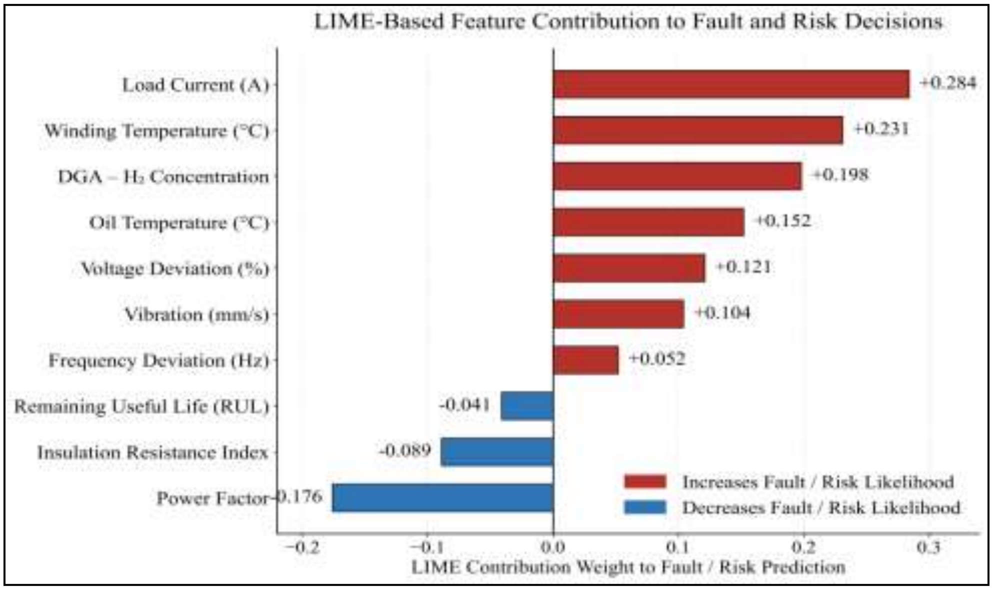


**Figure 8: LIME-Based Feature Contribution to Fault and Risk Decisions**

The figure 8 represents the impact of individual electrical, equipment-condition features on selected fault and risk predictions. It provides local interpretability through the identification of features that are most predictive of the decision.

**Table 8: Risk-Based Maintenance Priority and Recommended Maintenance Actions**

| Failure Risk (%) | Fault Severity (%) | Degradation (%) | Asset Criticality | Maintenance Priority | Recommended Maintenance Action |
|---|---|---|---|---|---|
| 12.4 | 10.8 | 8.6 | Low | Low | Routine monitoring |
| 27.6 | 24.3 | 21.5 | Medium | Low | Condition monitoring |
| 41.8 | 39.6 | 37.2 | Medium | Medium | Detailed inspection |
| 58.3 | 55.7 | 52.4 | High | Medium | Preventive maintenance |
| 74.6 | 71.8 | 69.5 | High | High | Immediate maintenance |
| 89.2 | 86.7 | 84.3 | Critical | Very High | Urgent repair or replacement |

Table 8 shows maintenance priority according to risk of failure, severity of fault, degradation degree and criticality of equipment. The gradual rise in the priority of maintenance from low to very high is caused by the aggregate of risk factors and causes a need for increasing levels of maintenance from monitoring to maintenance or replacement.

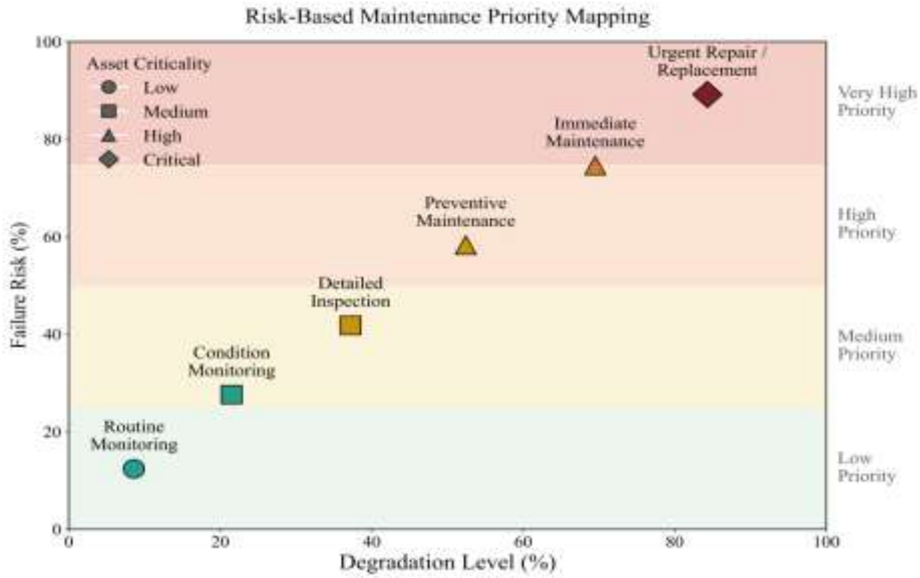


**Figure 9: Risk-Based Maintenance Priority Mapping**

The equipment maps in Figure 9 are used to establish the priority of maintenance through assessing failure probability and asset criticality. This is done to distinguish between assets of low importance and those which require urgent maintenance.

**Table 9: Comparative Performance of Existing Models and the Proposed Network**

| Model | Accuracy (%) | F1-Score (%) | Recall (%) | RMSE | ROC-AUC (%) |
|---|---|---|---|---|---|
| HML-XAI [1] | 91.84 | 91.26 | 90.73 | 0.184 | 92.31 |
| EL-PMU [3] | 93.21 | 92.47 | 92.05 | 0.165 | 94.18 |
| RF-XGBoost [6] | 93.68 | 93.14 | 92.62 | 0.157 | 94.72 |
| OML-FD [8] | 94.15 | 93.56 | 93.08 | 0.151 | 95.06 |
| LSTM-AE [15] | 94.62 | 94.03 | 93.71 | 0.143 | 95.41 |
| FA-Transformer [35] | 95.63 | 95.24 | 94.91 | 0.113 | 96.18 |
| RIGNNet (Proposed) | 96.23 | 95.91 | 95.64 | 0.098 | 96.78 |

Table 9 shows comparison of Hybrid ML Explainable Artificial Intelligence (HML-XAI), Ensemble Learning–Phasor Measurement Unit (EL-PMU), Random Forest–Extreme Gradient Boosting (RF-XGBoost), Optimized ML–Fault Diagnosis (OML-FD), Long Short-Term Memory–Autoencoder (LSTM-AE), Frequency-Aware Transformer (FA-Transformer) and the proposed RIGNNet is depicted in Table 9 in terms of Accuracy, F1-Score, Recall, RMSE and ROC-AUC. It can be seen from the results that the model RIGNNet produces the best results in terms of Accuracy at 96.23%, F1-Score at 95.91%, Recall at 95.64%, RMSE at 0.098 and ROC-AUC at 96.78% which proves its effectiveness in classifying and predicting the fault. The abbreviations are HML-XAI for Hybrid ML Explainable Artificial Intelligence, EL-PMU for Ensemble Learning Phasor Measurement Unit, RF-XGBoost for Random Forest Extreme Gradient Boosting, OML-FD for Optimized ML Fault Diagnosis, LSTM-AE for Long Short-Term Memory Autoencoder, FA-Transformer for Frequency-Aware Transformer and RIGNNet.

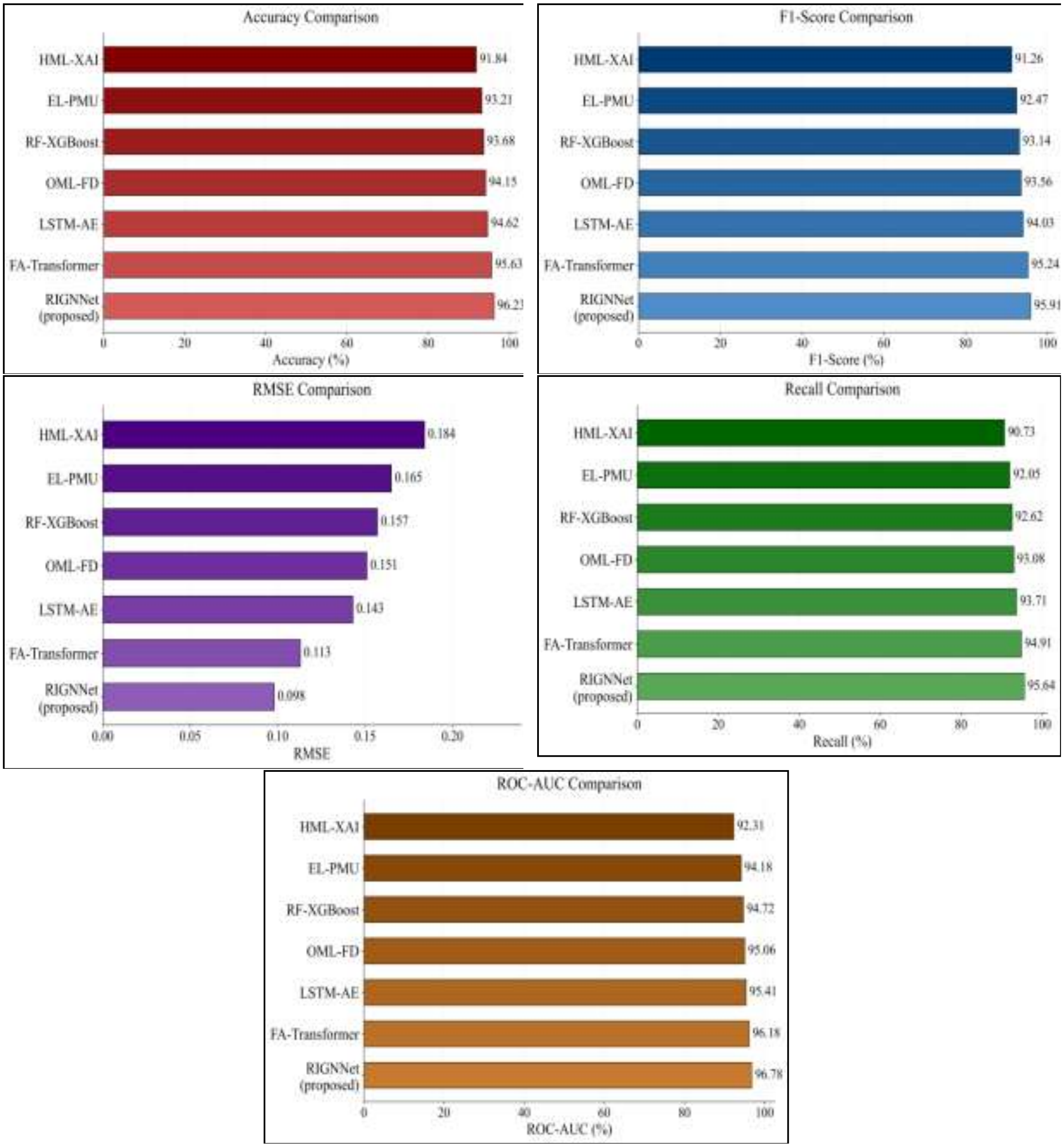


**Figure 10: Comparative Performance Analysis of Fault Diagnosis Models**

Figure 10 shows the comparative performance of the selected models with regard to accuracy, F1-score, recall, RMSE and ROC-AUC, where the actual values of all are represented by the height of bars. RIGNNet is the most accurate model with low RMSE among others.

### 4.1 Statistical Analysis

Statistical Data Analysis is used for analyzing the reliability and significance of the performance results of RIGNNet and the competing models. For statistical validation of the model, the statistical analysis is performed using confidence intervals, descriptive statistics, ANOVA and Mean ± SD.

#### 4.1.1 95% Confidence Interval analysis

This analysis, comparison is made among the 95% confidence interval estimates for model performances to gauge the level of certainty with the findings obtained. Confidence Interval refers to a range of values that can contain the real mean with 95% confidence.

**Table 10: 95% Confidence Interval Analysis of Model Performance**

| Model | Mean Performance (%) | Standard Error (SE) | 95% Confidence Interval (%) | Confidence Width (%) |
|---|---|---|---|---|
| HML-XAI [1] | 91.84 | 0.18 | 91.43–92.25 | 0.82 |
| EL-PMU [3] | 93.21 | 0.16 | 92.85–93.57 | 0.72 |
| RF-XGBoost [6] | 93.68 | 0.15 | 93.34–94.02 | 0.68 |
| OML-FD [8] | 94.15 | 0.14 | 93.83–94.47 | 0.64 |
| LSTM-AE [15] | 94.62 | 0.13 | 94.33–94.91 | 0.58 |
| FA-Transformer [35] | 95.63 | 0.12 | 95.36–95.90 | 0.54 |
| RIGNNet (Proposed) | 96.23 | 0.11 | 95.98–96.48 | 0.50 |

Table 10 shows the 95% confidence intervals for the performance of the models tested, along with the mean performance and its uncertainty for each value. It can be seen that RIGNNet has the lowest confidence interval of 0.50%, while the highest mean performance of 96.23% is the best one.

### 4.1.2 Descriptive Statistical Analysis

Descriptive statistics are used for summarizing the central tendency and variance of the performance achieved by the models under evaluation. Mean, Standard Deviation, Min and Max are all used for comparing the performance and stability of the models.

**Table 11: Descriptive Statistical Analysis of Model Performance**

| Model | Mean Performance (%) | Standard Deviation (%) | Minimum (%) | Maximum (%) |
|---|---|---|---|---|
| HML-XAI | 91.84 | 0.72 | 90.91 | 92.76 |
| EL-PMU | 93.21 | 0.65 | 92.38 | 94.05 |
| RF-XGBoost | 93.68 | 0.61 | 92.91 | 94.47 |
| OML-FD | 94.15 | 0.57 | 93.42 | 94.83 |
| LSTM-AE | 94.62 | 0.51 | 93.94 | 95.28 |
| FA-Transformer | 95.63 | 0.46 | 95.02 | 96.18 |
| RIGNNet (Proposed) | 96.23 | 0.39 | 95.71 | 96.68 |

In table 11 there are presented average value and standard deviation for the models together with minimum and maximum values found during the assessment process. RIGNNet demonstrates the smallest value of standard deviation (0.39%) as well as the largest value of mean (96.23%) among all the above which shows its superiority and stability.

### 4.1.3 ANOVA Study

ANOVA is applied to determine if the differences in performance of RIGNNet and the chosen models are statistically significant. This is done by comparing the mean performance among the models over multiple experimental runs. A value of 0.05 for alpha is adopted, where if p is less than 0.05, there is a significant difference. In general, there is statistical significance of RIGNNet prior to post hoc tests.

### 4.1.4 Mean Standard Deviation (SD) Analysis

The analysis on the mean ± SD highlights how the model performs on average and gives a brief description of the difference between the performance of the model on average compared to the average performance of the results. The SD is smaller and the mean larger with good-performing models.

**Table 12: Mean Standard Deviation Analysis of Model Performance**

| Model | Mean Performance (%) | Standard Deviation (%) | Mean ± SD (%) |
|---|---|---|---|
| HML-XAI | 91.84 | 0.72 | 91.84 ± 0.72 |
| EL-PMU | 93.21 | 0.65 | 93.21 ± 0.65 |
| RF-XGBoost | 93.68 | 0.61 | 93.68 ± 0.61 |
| OML-FD | 94.15 | 0.57 | 94.15 ± 0.57 |
| LSTM-AE | 94.62 | 0.51 | 94.62 ± 0.51 |
| FA-Transformer | 95.63 | 0.46 | 95.63 ± 0.46 |

| | | | |
|---|---|---|---|
| RIGNNet (Proposed) | 96.23 | 0.39 | 96.23 ± 0.39 |

Table 12 shows the mean ± SD value of the performance of the model is reported, showing the performance of the model and variability in the model. The best performance (96.23 ± 0.39%) with minimum variability is obtained through the RIGNNet modeling, which shows high performance and stability.

## 5. Discussion

The RIGNNet is evaluated in this section using ablation, practical deployment and limitation analyses to determine the effectiveness of the components, its operational applicability and implementation limitations. These analyses enable a comprehensive assessment of how the proposed model can perform, how it can be deployed and what are the practicalities.

### 5.1 Ablation study

The ablation study involves comparing and quantifying the contribution of each of the individual components by comparing RIGNNet to configurations that remove individual components. This analysis is used to determine the importance of each component, as well as to validate the overall RIGNNet configuration.

**Table 13: Ablation Analysis of RIGNNet Components**

| Configuration | Accuracy (%) | F1-Score (%) | Recall (%) | RMSE | ROC-AUC (%) |
|---|---|---|---|---|---|
| Without InceptionTime | 92.84 | 92.31 | 91.96 | 0.121 | 93.74 |
| Without GRU | 93.47 | 93.02 | 92.58 | 0.116 | 94.21 |
| Without N-BEATS | 94.18 | 93.76 | 93.35 | 0.109 | 94.86 |
| Without LightGBM | 93.91 | 93.48 | 93.06 | 0.112 | 94.53 |
| Without RBMD | 95.02 | 94.67 | 94.31 | 0.104 | 95.61 |
| Complete RIGNNet | 96.23 | 95.91 | 95.64 | 0.098 | 96.78 |

Table 13 analyses the contributions of individual RIGNNet modules by eliminating each module and comparing the performances. The complete RIGNNet yields the highest value for Accuracy, F1-Score, Recall and ROC-AUC, while yielding the lowest RMSE, indicating the contributions of all the modules.

### 5.2 Practical deployment Analysis

The practical deployment analysis evaluates the ability of RIGNNet to be deployed for real-time fault diagnosis and predictive maintenance of smart electrical power systems. The integrated architecture allows easy processing of electrical measurements and equipment-condition information, with early fault detection and equipment degradation prediction and failure risk estimation. It is modular in design and can be used on a wide range of equipment such as transformers, transmission lines, circuit breakers and power cables. This yields actionable priorities and explanations to operators of the power system based on the risk levels. The resulting risk-based priorities and LIME explanations are actionable and transparent support for the operators of the power system.

### 5.3 Limitation of Algorithm

High-quality, continuous and sufficiently diverse condition monitoring data is required for reliable fault diagnosis and degradation prediction in RIGNNet. The whole system is implemented by the combination of InceptionTime, GRU, N-BEATS and LightGBM, which makes the implementation and computational complexity much more difficult than integrating a single model. The performance of the model might deteriorate considerably when operating conditions and/or equipment parameters are significantly different from those at training time. In addition, the explanations that LIME generates increase the computational cost when decision making in real-time.

## 6. Conclusion

RIGNNet is a package that integrates the packages InceptionTime, GRU, N-BEATS, LightGBM, RBMD and LIME for fault diagnosis and predictive maintenance (PdM) in smart electrical power systems. The methodology can be applied to identify multi-scale fault-features, understand the temporal condition, forecast the degradation, characterizing the faults, determining the fault severity, assessing failure risk, prioritizing maintenance and taking meaningful decisions. Experimental results on the tested existing approaches showed that RIGNNet has an F1-Score of 95.91%, Recall of 95.64%, ROC-AUC of 96.78% and an RMSE of 0.098 which was superior. It was able to detect progressive degradation of assets through degradation and risk analyses and to prioritize maintenance activities; LIME provided transparent explanations of feature-level model predictions. The integrated architecture was also effective and the results of the ablation were confirmed. In summary, RIGNNet promotes accurate, proactive, risk-aware and explainable power-system asset management, which can used to prevent unexpected failures and unnecessary maintenance interventions. Future research will focus on multimodal sensing, on boarding additional multi-asset datasets, online learning, uncertainty-aware prediction, on boarding edges, on boarding digital twins and federated learning and automated maintenance scheduling for large-scale real-time power-system management.

## Reference


1. Aslan, E., Özüpak, Y., Alpsalaz, F., & Elbarbary, Z. M. (2025). A hybrid machine learning approach for predicting power transformer failures using internet of things-based monitoring and explainable artificial intelligence. *IEEE Access*, *13*, 113618-113633. https://doi.org/10.1109/ACCESS.2025.3583773
2. Ashraf, M. W., Avanija, J., Ballireddy, T. R., Singh, A. R., Bajaj, M., & Rubanenko, O. (2026). Artificial intelligence-driven dynamic optimization for predictive maintenance and cybersecurity in smart power distribution networks. *Energy Exploration & Exploitation*, *44*(2), 771-798. https://doi.org/10.1177/01445987251386897
3. Bin Akter, S., Sarkar Pias, T., Rahman Deeba, S., Hossain, J., & Abdur Rahman, H. (2024). Ensemble learning based transmission line fault classification using phasor measurement unit (PMU) data with explainable AI (XAI). *Plos one*, *19*(2), e0295144. https://doi.org/10.1371/journal.pone.0295144
4. Poursaeed, A. H., & Namdari, F. (2025). Explainable AI-driven quantum deep neural network for fault location in DC microgrids. *Energies*, *18*(4), 908. https://doi.org/10.3390/en18040908
5. Biswas, A. K., Ahamed, M. F., Shafi, F. B., Murugappan, M., Chowdhury, M. E., Nagalingam, R., & Lawrence, T. S. (2026). Hybrid CNN-decision tree framework for efficient transmission line fault detection and classification: an XAI-based approach. *Scientific Reports*. https://doi.org/10.1038/s41598-026-45514-0
6. Rengasamy, P., & Rajesh, R. (2025). Explainable artificial intelligence framework for wind turbine fault detection using random forest-extreme gradient boosting hybrid model. *Results in Engineering*, 107446. https://doi.org/10.1016/j.rineng.2025.107446
7. Giri, T., Thapa, B. B., Paneru, B., & Paneru, B. (2026). An XAI-driven CNN-transformer model for transmission line fault detection and classification. *Energy Reports*, *15*, 108929. https://doi.org/10.1016/j.egyr.2025.108929
8. Najafzadeh, M., Pouladi, J., Daghigh, A., Beiza, J., & Abedinzade, T. (2024). Fault detection, classification and localization along the power grid line using optimized machine learning algorithms. *International Journal of Computational Intelligence Systems*, *17*(1), 49. https://doi.org/10.1007/s44196-024-00434-7
9. Hariharan, V. K., Geetha, A., Granelli, F., & Nair, M. G. (2025). Machine learning techniques for fault detection in smart distribution grids. *Energies*, *18*(19), 5179. https://doi.org/10.3390/en18195179
10. Ness, S. (2025). Enhancing smart grid reliability: Fault detection in phasor measurement unit images with deep learning. *IEEE Access*, *13*, 69257-69268. https://doi.org/10.1109/ACCESS.2025.3561587
11. Riaz, Z., Khan, A. Q., Habib, S., Saad, M., Zaman, F., Alghamdi, S. M., & Yousef, A. (2026). Hybrid machine learning and deep learning framework for multi-stage fault diagnosis in modern power systems. *Energy Reports*, *16*, 109558. https://doi.org/10.1016/j.egyr.2026.109558
12. Kaushal, R. K., Raveendra, K., Nagabhooshanam, N., Azam, M., Brindha, G., Anand, D., ... & Rambabu, K. (2025). Fault prediction and awareness for power distribution in grid connected res using hybrid machine learning. *Electric Power Components and Systems*, *53*(14), 1744-1765. https://doi.org/10.1080/15325008.2024.2337217
13. Vaish, R., & Dwivedi, U. D. (2024). Performance and adaptability testing of machine learning models for power transmission network fault diagnosis with renewable energy sources integration. *IEEE Access*, *12*, 94092-94115. https://doi.org/10.1109/ACCESS.2024.3425057
14. Liu, C., Ding, L., & Yu, H. (2025). Intelligent Fault Detection in Power Grids Using Deep Learning Algorithms. *IEEE Access*. https://doi.org/10.1109/ACCESS.2025.3606856

15. Hossain, M. I., Anonto, H. Z., Riyad, T., Shufian, A., Hossain, M. S., & Pathik, B. B. (2026). Adaptive fault diagnosis in power transmission lines using deep learning and LSTM autoencoders for enhancing grid reliability. *International Journal of Electrical Power & Energy Systems*, *174*, 111458. https://doi.org/10.1016/j.ijepes.2025.111458
16. Attallah, O., Ibrahim, R. A., & Zakzouk, N. E. (2025). A lightweight deep learning framework for transformer fault diagnosis in smart grids using multiple scale CNN features. *Scientific reports*, *15*(1), 14505. https://doi.org/10.1038/s41598-025-96290-2
17. Yu, Q., Guan, T., Tian, A., Si, M., Qi, B., Jiang, Y., ... & Zhang, W. (2024). Fault diagnosis based on tensor computing and meta-learning for smart grid and power communication network. *Electronics*, *13*(9), 1655. https://doi.org/10.3390/electronics13091655
18. Elkheir, E. S. I. A., Abd-Allah, M. A., Hussien, S. A., & Omar, A. I. (2026). Real-time microgrid fault management: Leveraging hybrid deep learning for superior detection and classification performance. *IEEE Access*, *14*, 9606-9623. https://doi.org/10.1109/ACCESS.2026.3654266
19. Senapati, M., Panigrahi, P., Mohanty, A., & Das, S. R. (2026). Hybrid Deep Learning and Kalman Filtering for Reactive Power Fault Diagnosis in Smart Microgrids. *IEEE Access*. https://doi.org/10.1109/ACCESS.2026.3681913
20. Zhong, J., Chen, Y., Gao, J., & Lv, X. (2024). Drone image recognition and intelligent power distribution network equipment fault detection based on the transformer model and transfer learning. *Frontiers in Energy Research*, *12*, 1364445. https://doi.org/10.3389/fenrg.2024.1364445
21. Zhang, Y., Guo, Y., Lin, Q., Fan, Z., Qiu, S., Wu, X., & Fang, X. (2026). Graph-augmented fault diagnosis in power systems with imbalanced text data: A knowledge extraction and agent-based reasoning framework. *Technologies*, *14*(3), 181. https://doi.org/10.3390/technologies14030181
22. Yang, M., Wei, L., Qiu, P., Hu, G., Liu, X., He, X., ... & Zhao, X. (2025). Research on fault diagnosis of high-voltage circuit breakers using Gramian-Angular-Field-based dual-channel convolutional neural network. *Energies*, *18*(14), 3837. https://doi.org/10.3390/en18143837
23. Xiao, F., Shang, X., Li, Q., Zhan, Y., Li, R., Ai, Q., & Zhang, Y. (2026). Distribution Network Fault Diagnosis with Noise-Assisted Multivariate Empirical Mode Decomposition and a Modified Multiple Branch Convolutional Neural Network. *Energies*, *19*(9), 2187. https://doi.org/10.3390/en19092187
24. Jachymczyk, U., Knap, P., & Lalik, K. (2024). Improved intelligent condition monitoring with diagnostic indicator selection. *Sensors*, *25*(1), 137. https://doi.org/10.3390/s25010137
25. Abdolahi, M., Song, W., & Yazdani-Asrami, M. (2025). Intelligent condition monitoring of power cables using advanced machine learning models. *Results in Engineering*, 108371. https://doi.org/10.1016/j.rineng.2025.108371
26. Hämäläinen, A., Karhinen, A., Miettinen, J., Dahl, Z., & Viitala, R. (2025). Rapid deployment of deep learning-based condition monitoring for rotating machines. *IEEE Access*, *13*, 192023-192044. https://doi.org/10.1109/ACCESS.2025.3627885
27. Long, F., Hong, L., & Gao, Z. (2026). Transmission Line Fault Diagnosis Based on Time–Frequency-Domain Recurrence Plots and CNN-BiGRU-Attention. *Processes*, *14*(13), 2196. https://doi.org/10.3390/pr14132196
28. Li, L., & Wu, W. (2026). Research on Fault Type Identification for Distribution Networks with Distributed Power Sources Based on Improved CNN-BiGRU. *Sensors*, *26*(12), 3947. https://doi.org/10.3390/s26123947
29. Zhang, W., Cheng, M., Xiang, Q., & Li, Q. (2025). Enhancing short-term load forecasting through K-Shape clustering and deep learning integration. *IEEE Access*, *13*, 30817-30832. https://doi.org/10.1109/ACCESS.2025.3541574
30. Aravanis, T., & Kanavos, A. (2026). Comparative Evaluation of Deep Learning Architectures for Electricity Demand Forecasting. *Mathematics*, *14*(5), 827. https://doi.org/10.3390/math14050827
31. Nawaz, R., Wadood, A., Mehmood, K. K., Bukhari, S. B. A., Albalawi, H., Alatwi, A. M., & Sajid, M. (2025). Gradient boosting feature selection for integrated fault diagnosis in series-compensated transmission lines. *IEEE Access*, *13*, 63640-63670. https://doi.org/10.1109/ACCESS.2025.3558796
32. Nawaz, R., Qamar, A., Wadood, A., & Albalawi, H. (2026). Consensus-based feature selection and Bayesian-optimized stacking ensembles for comprehensive fault diagnosis in series-compensated ultra-high-voltage power systems. *Scientific Reports*. https://doi.org/10.1038/s41598-026-49195-7
33. Oliveira, J., Passos, D., Carvalho, D., Melo, J. F., Silva, E. G., & de Mattos Neto, P. S. (2024). Improving electrical fault detection using multiple classifier systems. *Energies*, *17*(22), 5787. https://doi.org/10.3390/en17225787

34. Chen, Y., Tang, Z., Weng, X., He, M., Zhou, S., Liu, Z., & Jin, T. (2024). A diagnostic method for open-circuit faults in DC charging stations based on improved S-transform and LightGBM. *Energies*, *17*(2), 404. https://doi.org/10.3390/en17020404
35. Choi, Y., & Joe, I. (2025). A frequency-aware transformer for multiscale fault diagnosis in electrical machines. *IEEE Access*. https://doi.org/10.1109/ACCESS.2025.3596859